Journal of Integrative Neuroscience

J. Integr. Neurosci. **2022**; 21(6): 157
https://doi.org/10.31083/j.jin2106157

Original Research

Assessment of Morphological Features and Imaging Characteristics of Patients with Intracranial Artery Dissection: A High-Resolution MRI Study

Qin Wu[1], Yigang Liu[2], Boheng Duan[3], Xiaoru Yuan[1], Zheng Zuo[1], Feng Ouyang[1], Mingxue Yin[1], Ye Chen[1], Xianjun Zeng[1,*]

[1]Department of Radiology, The First Affiliated Hospital of Nanchang University, 330006 Nanchang, Jiangxi, China
[2]Department of Ultrasound, Jiangxi Cancer Hospital, 330029 Nanchang, Jiangxi, China
[3]Class 211, Innovation Experiment, Nanchang University, 330031 Nanchang, Jiangxi, China
*Correspondence: xianjun-zeng@126.com (Xianjun Zeng)
Academic Editor: Giovanni Grasso
Submitted: 27 January 2022 Revised: 28 April 2022 Accepted: 29 April 2022 Published: 20 September 2022

Abstract

Background: Intracranial artery dissection (IAD) is a pathological dissection of the arterial wall. .However, the morphological features and imaging characteristics of patients with intracranial artery dissection (IAD) remain poorly understood. **Methods**: The study reports on 70 IAD patients (30 culprit and 40 non-culprit). All participants underwent high-resolution magnetic resonance imaging (HR-MRI) scans. The morphological features and imaging characteristics of artery dissection were carefully investigated. Demographics and clinical characteristics of culprit and non-culprit patients were also collected. Apparent differences between the two groups, which could be used as biomarkers for ischemic event caused by the culprit dissection, were identified by receiver operating characteristic (ROC) curve analysis. **Results**: The IAD patients studied could be classified into five different types on the basis of morphological features: classical dissection (n = 31), fusiform aneurysm (n = 2), long dissected aneurysm (n = 9), dolichoectatic dissecting aneurysm (n = 6), and saccular aneurysm (n = 22). The direct sites of artery dissection (double lumen and intimal flap) can be seen in most IAD patients on HR-MRI. Additionally, the presence of hypertension, double lumen and intimal flap were associated with culprit lesions and might be considered biomarkers for the ischemic event caused by the culprit dissection. **Conclusions**: Analysis showed that HR-MRI allowed easy visualization of abnormal morphology of artery dissection lesions. This was of great significance for the diagnosis of IAD and gave a better understanding of its pathophysiological mechanism.

Keywords: intracranial artery dissection; high-resolution magnetic resonance imaging; ischemic event

1. Introduction

Intracranial artery dissection (IAD) is a pathological dissection of the arterial wall [1,2]. It involves the arterial intima, forming subintimal hematoma and expands between the arterial intima and arterial media [3]. IAD can occur in any part of the intracranial artery, mainly in the latter circulation in Asia, but mainly in the former circulation in Western countries [4]. It has been reported that the incidence of IAD in European population is less than 10% of carotid artery dissection. However, IAD accounts for 67% to 90% of all CAD in East Asian populations [5]. There are more male patients with IAD than females, with an average age of 50.4 years. The site of IAD is more common in the posterior circulation than the anterior circulation, with the V4 segment of the vertebral artery the most common site. IAD in the posterior circulation usually causes subarachnoid hemorrhage, which is accompanied by headache and neck pain, while patients with IAD in anterior circulation mostly have symptoms of ischemia [6,7]. Until now, very little is known about the etiology of IAD. Hypertension, diabetes, hyperlipidemia, moyamoya disease, oral contraceptives, migraine and recent history of infection are considered to be predisposing factors for IAD [8,9].

Due to the lack of specificity of clinical manifestations, the diagnosis of IAD mainly depends on imaging examination. The diameter of the intracranial artery is thin and the aisle is also tortuous. Low spatial resolution of intracranial artery therefore limits effective inspection methods, increasing the difficulty of diagnosis. Digital subtraction angiography (DSA), magnetic resonance imaging (MRI) and computed tomography angiography (CTA) are common imaging methods for IAD [10,11]. With the advantages of fast imaging and the ability to provide clinicians with dynamic vascular luminal conditions throughout its course, DAS currently provides the best methodology for the clinical diagnosis of IAD. However, it should be noted that DSA is an invasive inspection method, which may cause trauma to subjects during the implementation process. Further, the risk of complications with DSA is relatively high, which is not conducive to the active acceptance and cooperation of the examination. The characteristic imaging signs of IAD with DSA are the intimal flap and

double lumen, but they are only seen in a low number of patients [12]. Additionally, DSA cannot directly show the wall of the involved artery, so patients with no significant changes in the diameter of the artery may be missed. For this reason, fusiform expansion or gradual stenosis shown on DSA should be distinguished from atherosclerotic disease.

Craniocerebral MRI better reveals blood vessel wall, lumen and intramural hematoma than DSA. High-resolution MRI (HR-MRI) is a clinical imaging evaluation technology that has emerged in recent years. Compared with conventional MRI, HR-MRI mainly uses black blood sequence based on fast spin echo sequence and bright blood sequence based on gradient echo sequence [13,14]. Black blood technology eliminates the signals of blood, extraluminal cerebrospinal fluid and perivascular fat, while achieving high-resolution images of the vascular wall. Bright blood technology clearly shows the boundary between blood and the vascular wall and assists with observation of the fine structure of the lumen and vascular wall lesions, so as to assist analysis of the etiology. HR-MRI is a technique that can effectively inhibit the signals of flowing blood in vessels, thereby providing the operator with a static tissue image of the vessel wall This is helpful for evaluating the pathological shape of the arterial vessel wall [15]. Further, by reducing the layer thickness and voxel size, HR-MRI provides high spatial resolution images for more accurate evaluation. However, HR-MRI has rarely been applied for the analysis of patients with IAD, so this study aimed to show the morphological features and imaging characteristics of IAD patients by use of HR-MRI and demonstrate the clinical value of HR-MRI for IAD patients.

2. Materials and Methods

2.1 Subjects

For the current study, IAD patients who had undergone HR-MRI in the First Affiliated Hospital of Nanchang University from October 2018 to October 2021 were selected, along with their medical records and the results of imaging examinations and laboratory tests. The study was approved by the Medical Ethics Committee of the First Affiliated Hospital of Nanchang University. The inclusion criteria for IAD patients included: (1) Meeting the diagnostic criteria of IAD [16]; (2) Being over the age of 18 years; (3) Having no liver or kidney disease; and (4) Having no contraindications for MRI examination. The exclusion criteria were: (1) Cerebrovascular diseases, including intracranial or extracranial atherosclerosis with stenosis $\geq$50%, vasculitis, moyamoya disease, and fibromuscular dysplasia; (2) Chronic ischemic symptoms ($>$12 weeks); (3) Severe heart disease or suspected cardiogenic stroke; (4) A previous history of stroke or transient ischemic attack; (5) Serious coagulation dysfunction; and (6) A history of mental illness such as schizophrenia or bipolar disorder. IAD patients underwent HR-MRI examination within seven days of hospitalization. Demographic and clinical characteristics were collected, including age, gender, hypertension, hyperlipidemia, diabetes and smoking. Research was performed according to the principles of medical ethics. All methods were performed under the guidelines of the Declaration of Helsinki. Additionally, all participants were informed of the goals, procedures and potential risks and signed and informed consent.

2.2 HR-MRI Acquisition

A 3-Tesla MR scanner with a 32-channel head coil (Magnetom skyra, Siemens, Germany) was utilized to obtain brain MR images. All participants were asked to keep their heads still, close their eyes and stay awake for the duration of their MRI scan. The scanning sequence included three-dimensional time-of-flight magnetic resonance angiography (3D-TOF MRA) and three dismensional-T1 weighted sampling perfection with application of optimized contrasts using different flip angle evolution (3D-T1WI SPACE). The parameters for 3D-TOF MRA and 3D-T1WI SPACE have been described elsewhere [17,18]. After the 3D-TOF MRA and 3D-T1WI SPACE scanning sequences, the patient's cubital vein was connected to a high-pressure syringe and 20 mL of gadoterate meglumine and 30 mL of normal saline were injected. After five minutes, scanning using the 3D-SPACE-T1WI sequence was repeated.

2.3 Imaging Analysis

HR-MRI results were independently analyzed by two senior radiologists. When their opinions differed, a more senior doctor was consulted. Then three doctors then discussed the case and reached a consensus opinion of the diagnosis. The presence of ischemic stroke was judged by cerebrovascular and neurological symptoms and traditional MRI. IAD patients without typical cerebrovascular symptoms and dissected vessels showing a normal MRI signal were considered non-culprit. Alternatively they were considered as culprit.

Two imaging physicians searched for evidence of IAD in each patient HR-MRI image and recorded the following information: location of the lesion, shape of the lumen, presence or absence of hematoma, signal of hematoma, presence or absence of a double lumen, intimal flap, intraluminal thrombus enhancement and intimal flap enhancement, the grade of vessel wall enhancement and the type of the dissection. Representative cases are shown in Fig. 1.

2.4 Statistical Analysis

Data were analyzed with SPSS software (version 22.0; Armonk, New York, USA). Chi-square and Fisher's exact tests were applied to categorical data and the independent Student's *t*-test was utilized for continuous data. The differences in the serological indicators between the culprit and non-culprit groups were also calculated by independent Student's *t*-test. Data were presented as the mean $\pm$ SD. A

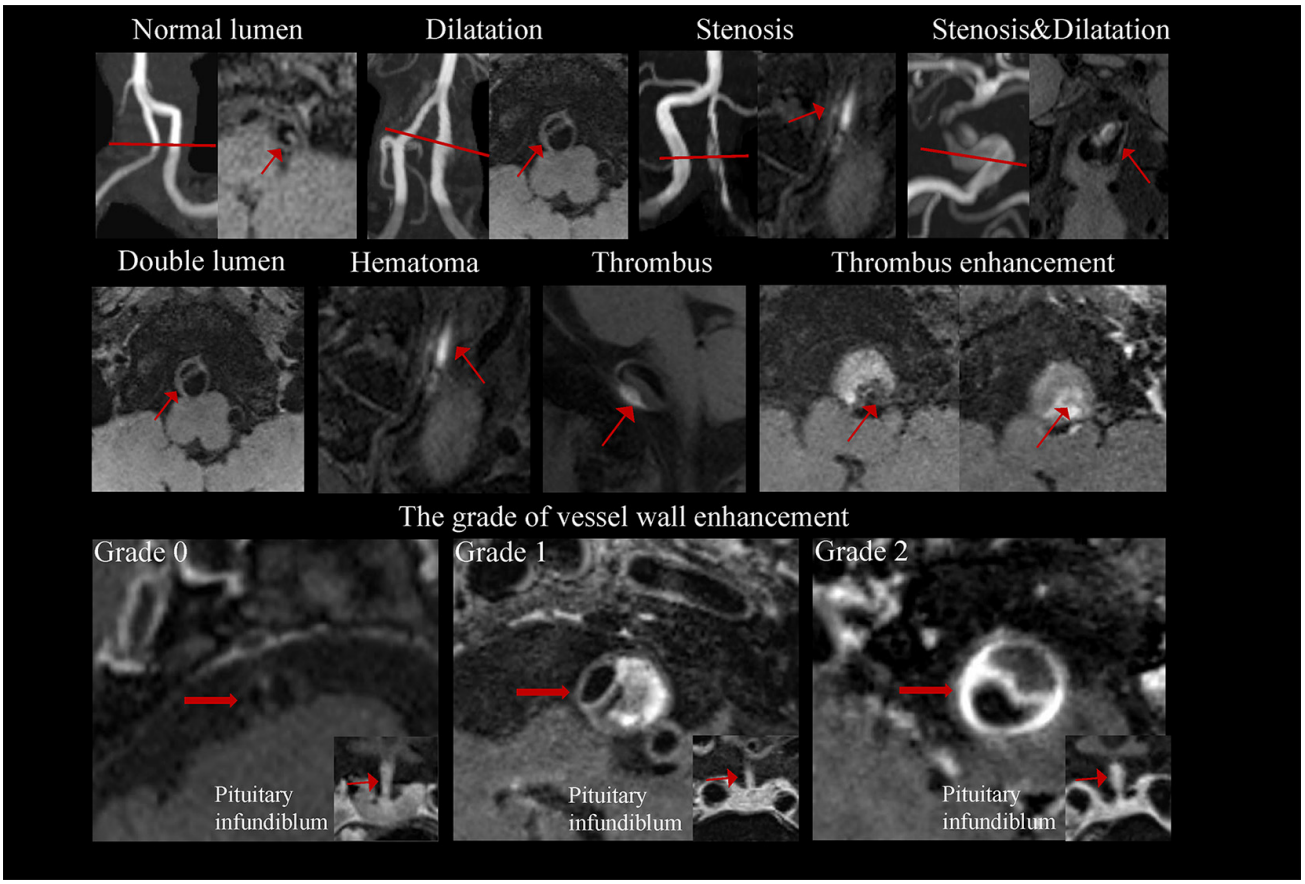

Fig. 1. Typical HR-MRI of IAD with different morphological and compositional features. Abbreviations: HR-MRI, high-resolution magnetic resonance images; IAD, intracranial artery dissection.

$p < 0.05$ was considered statistically significant. It was hypothesized that differences in demographics and clinical characteristics could be used as biomarkers for diagnosis of culprit. The receiver operating characteristic (ROC) curve method was subsequently used to test this hypothesis and was generated to analyze and identify ischemic events caused by the culprit dissection.

3. Results

3.1 Demographics and Clinical Characteristics

A total of 70 patients (49 male and 21 female) were recruited for this study. Among them, 48 patients (68.6%) were diagnosed with hypertension, 7 (10%) with hyperlipidemia and 5 (7.14%) with diabetes. There were also 10 patients (14.3%) with a history of drinking and 14 patients (20%) with a history of smoking (20%). According to morphological features, IAD patients involved in this study could be classified into five different types. No statistical significances were observed in terms of age, gender, hyperlipidemia, diabetes, drinking and smoking. However, the distribution of patients with hypertension and clinical symptoms in the five different types of IAD were statistically different. More details are given in Table 1 and Fig. 2.

3.2 Morphological Features and Imaging Characteristics of HR-MRI

In this study, IAD was divided into five types: classical dissection (Type I; $n = 31$ (44.3%)), fusiform aneurysm (Type II; $n = 2$ (2.8%)), long dissected aneurysm (Type III; $n = 9$ (12.9%)), dolichoectatic dissecting aneurysm (Type IV; $n = 6$ (8.6%)) and saccular aneurysm (Type V; $n = 22$ (31.4%)). Classical dissection was the most common, followed by saccular aneurysm and long dissected aneurysm. As for location of lesions, almost three-quarters of lesions were found to occur in the vertebral artery (74.3%). Double lumen and intimal flap on HR-MRI, which were direct signs of IAD, were visible in 82.8% and 84.3% of IAD patients, respectively. Further, 28.6% and 71.4% of patients, respectively, showed enhanced thrombosis and endometrial flap enhancement. More detailed information is displayed in Table 2.

3.3 Factors Associated with Culprit and Non-Culprit Lesions

The ischemic event caused by the culprit dissection can seriously affect the prognosis of IAD patients. There were 30 patients with culprit and 40 patients without culprit in this study. Serological indicators and imaging results of

Table 1. Demographics and clinical characteristics of IAD patients among the five types.

	Mean ± SD or n (%)					*p* value
	Type I	Type II	Type III	Type IV	Type V	
Patients number	31	2	9	6	22	
Male/Female	18/13	1/1	6/3	5/1	19/3	0.185
Age	53.45 ± 11.03	56.00 ± 1.41	57.33 ± 11.36	62.00 ± 6.42	55.82 ± 8.72	0.391
Hypertension	20/11	0/2	8/1	6/0	14/8	0.020*
Hyperlipidemia	4/27	0/2	1/8	1/5	1/21	0.764
Diabetes	2/29	0/2	2/7	0/6	1/21	0.474
Drinking	5/26	0/2	1/8	1/5	3/19	0.937
Smoking	7/24	0/2	0/9	1/5	6/16	0.219
TG (mmol/L)	1.35 ± 0.76	1.08 ± 0.83	1.46 ± 0.52	1.00 ± 0.21	1.41 ± 0.65	0.660
LDL (mmol/L)	2.44 ± 0.83	2.28 ± 1.22	2.66 ± 1.36	2.54 ± 0.85	2.75 ± 0.78	0.756
HDL (mmol/L)	1.28 ± 0.28	0.91 ± 0.01	1.14 ± 0.31	1.14 ± 0.57	1.14 ± 0.35	0.268
Confirmed by DSA	27 (87.1)	2 (100.0)	9 (100.0)	6 (100.0)	22 (100.0)	0.146
Clinical symptoms	29/2	0/2	8/1	6/0	21/1	0.020*

Notes: *: $p < 0.05$ was set as statistical level. Abbreviations: IAD, intracranial artery dissection; TG, triglycerides; LDL, low density lipoprotein; HDL, high density lipoprotein; DSA, digital subtraction angiography.

Table 2. Morphological features and imaging characteristics of the dissection among the five types.

	Mean ± SD or n (%)					*p* value
	Type I	Type II	Type III	Type IV	Type V	
Location						0.467
MCA	3 (9.7)	1 (50.0)	0 (0)	0 (0)	1 (4.5)	
VA	23 (74.2)	1 (50.0)	5 (55.6)	6 (100.0)	17 (77.3)	
BA	4 (12.9)	0 (0)	4 (44.4)	0 (0)	3 (13.6)	
PCA	0 (0)	0 (0)	0 (0)	0 (0)	1 (4.5)	
ACA	1 (3.2)	0 (0)	0 (0)	0 (0)	0 (0)	
Lumen shape						0.062
Normal	4 (12.9)	0 (0)	0 (0)	0 (0)	1 (4.5)	
Stenosis	10 (32.2)	0 (0)	1 (11.1)	2 (33.3)	12 (54.5)	
Dilatation	17 (54.8)	2 (100.0)	6 (66.7)	3 (50.0)	9 (40.9)	
Stenosis and dilatation	0 (0)	0 (0)	2 (22.2)	1 (16.7)	0 (0)	
Hematoma	5 (16.1)	0 (0)	6 (66.7)	6 (100.0)	10 (45.5)	<0.001*
Hematoma signal on T1WI						0.008*
No enhancement	26 (83.9)	2 (100.0)	3 (33.3)	0 (0)	12 (54.5)	
Isointensity	0 (0)	0 (0)	2 (22.2)	2 (33.3)	2 (9.1)	
Hyperintensity	3 (9.7)	0 (0)	2 (22.2)	1 (16.7)	5 (22.7)	
Hypointensity	2 (6.4)	0 (0)	1 (11.1)	3 (50.0)	3 (13.6)	
Heterogeneous intensity	0 (0)	0 (0)	1 (11.1)	0 (0)	0 (0)	
Double lumen	28 (90.3)	2 (100.0)	7 (77.7)	3 (50.0)	18 (81.8)	0.222
Intimal flap	27 (87.1)	2 (100.0)	6 (66.6)	5 (83.8)	19 (86.4)	0.617
Thrombus enhancement	2 (6.5)	0 (0)	0 (0)	5 (83.8)	13 (59.1)	<0.001*
Intimal flap enhancement	24 (77.4)	2 (100.0)	5 (55.6)	3 (50.0)	16 (72.7)	0.383
Vessel wall enhancement grade						0.108
No enhancement	0 (0)	0 (0)	0 (0)	0 (0)	0 (0)	
Enhancement	4 (12.9)	0 (0)	2 (22.2)	0 (0)	0 (0)	
Obvious enhancement	27 (87.1)	2 (100.0)	7 (77.7)	6 (100.0)	22 (100.0)	

Notes: *: $p < 0.05$ was set as statistical level. Abbreviations: MCA, middle cerebral artery; VA, vertebral artery; BA, basilar artery; PCA, posterior cerebral artery; ACA, anterior cerebral artery; TIWI, T1 weighted image.

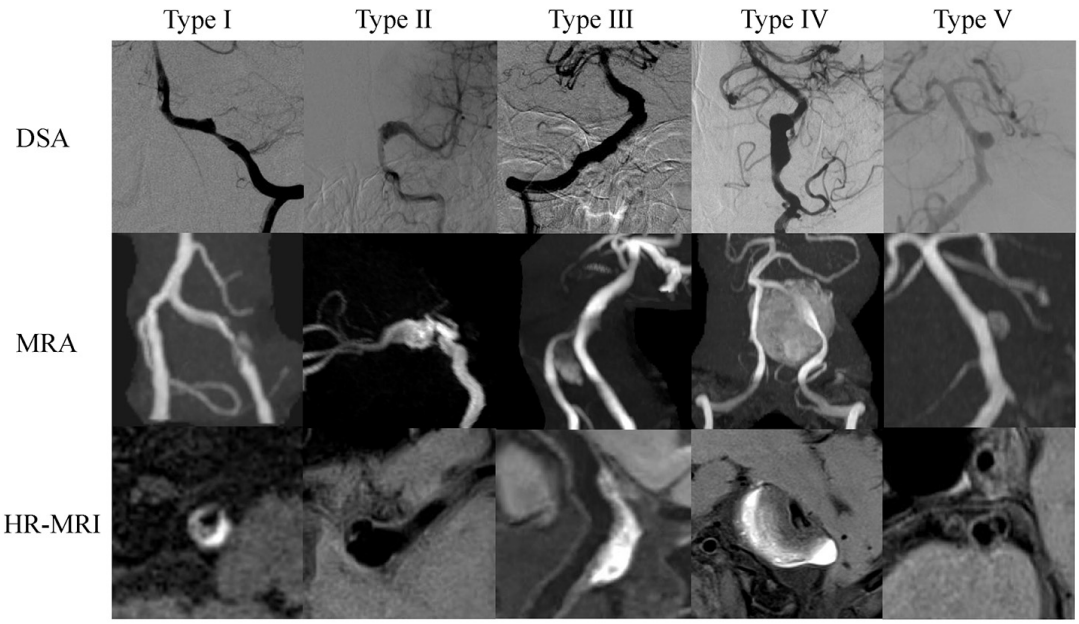

Fig. 2. Typical manifestations of different types of IAD on DSA, MRA and HR-MRI. Type I: Classical dissection; Type II: Fusiform aneurysm; Type III: Long dissected aneurysm; Type IV: Dolichoectatic dissecting aneurysm; Type V: Saccular aneurysm. Abbreviations: IAD, intracranial artery dissection; DSA, digital subtraction angiography; MRA, magnetic resonance angiograpgy; HR-MRI, high-resolution magnetic resonance images.

the two culprit and non-culprit patients were analyzed in an attempt to find risk factors for an ischemic event caused by culprit dissection. The results displayed remarkable differences in the percentage of patients with hypertension, double lumen and intimal flap ($p < 0.05$). A detailed comparison is given in Table 3. Representative cases of culprit and non-culprit dissections are displayed in Fig. 3.

3.4 ROC Analysis

Following computational analysis, it was observed that the presence of hypertension, double lumen and intimal flap might be useful for the diagnosis of ischemic events caused by culprit dissection. Further, the area under curves (AUCs) of hypertension, double lumen and intimal flap were 0.604, 0.671 and 0.658, respectively. Additionally, the AUCs of combinations of hypertension + double, hypertension + intimal flap, lumen + intimal flap and hypertension + double + intimal flap were respectively, 0.753, 0.717, 0.811 and 0.866, indicating high values for prediction of ischemic events caused by culprit dissection (Fig. 4).

4. Discussion

IAD, including dissection and dissection aneurysm, is a primary cause of stroke in young and middle-aged people [19]. IAD can lead to severe cerebral ischemia or cerebral hemorrhage, so early diagnosis is particularly important. However, it is difficult to show the abnormal lumen structure of lesions by CTA and DSA, so the diagnosis of IAD remains a considerable challenge.

The application of HR-MRI in vascular-related diseases has attracted increasing attention in recent years. With the advantages of being non-invasive, high repeatability, high spatial resolution and providing multi-parameter imaging, HR-MRI has been used in previous studies for evaluating atherosclerotic diseases, ischemic stroke and moyamoya disease [20–22]. This technology provides information not only on the lumen, but also on the morphology and composition of the tube wall. In this study, it was shown that HR-MRI significantly assisted the visualization and characterization of IAD, which was also helpful in providing a greater in-depth understanding of IAD and its differentiation from other intracranial artery diseases.

Several characteristic patterns of HR-MRI in artery disease have been described. In unilateral middle cerebral artery inflammatory stenosis, HR-MRI has accurately determined the degree of intracranial artery stenosis and provided important diagnostic information for arterial inflammatory stenosis [23]. Additionally, the HR-MRI results of middle cerebral artery occlusion caused by intracranial atherosclerosis primarily manifested as eccentric involvement of the vessel wall with uneven signal intensity, while patients with moyamoya disease typically exhibited concentric involvement of the vessel wall with relatively uniform signal intensity [24,25]. HR-MRI was also considered to be a useful future tool for the differential diagnosis of moyamoya disease due to its value in assessing the pathological changes of blood vessel walls and understanding the fundamental mechanisms of the disease. A previous study

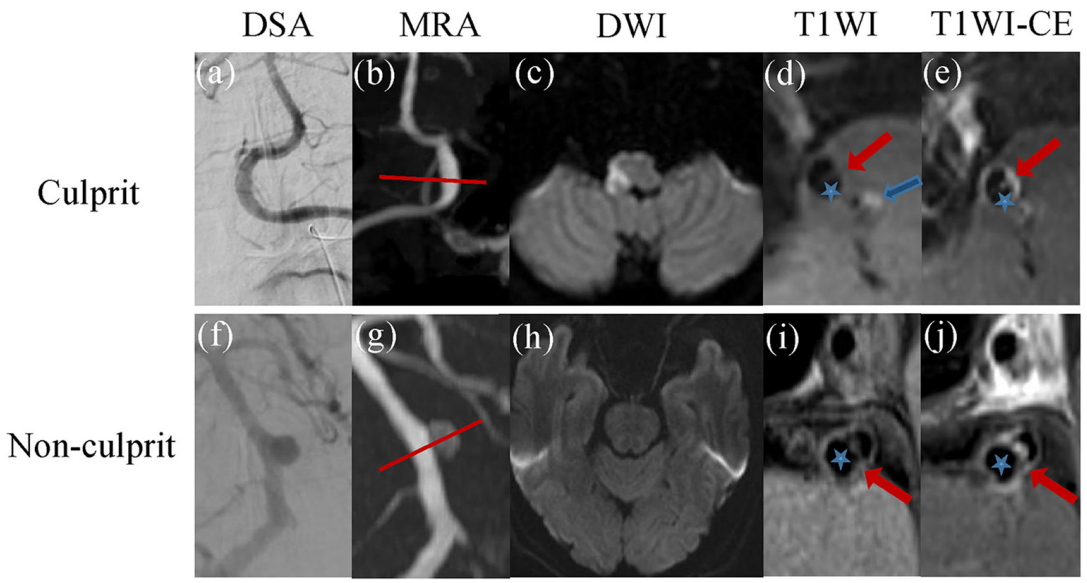

Fig. 3. The cases of IAD with culprit and non-culprit dissections. (a–e) A 48-year-old IAD patient with culprit dissection. DSA and MRA demonstrated local thickening in the V4 segment of the right vertebral artery and local stenosis in the V4 segment of the left vertebral artery (a,b). DWI confirmed acute cerebral infarction in the right medulla oblongata (c). HR-MRI showed double lumen (five-pointed star) and the intimal flap (red arrow) and intermural hematoma (blue arrow) (d). CE-T1 image showed enhanced intimal flap and vessel wall in the V4 segment of the right vertebral artery (e). (f–j) The case of 58-year-old IAD patient with non-culprit dissection. Both DSA and MRA showed the formation of basilar artery aneurysm (f,g). No obvious acute cerebral infarction was observed on DWI (h). HR-MRI showed double lumens (five-pointed star) and intimal flap (red arrow) in the basilar artery lesion (i). And CE-T1 image also displayed obviously enhanced intimal flap and vessel wall (j). Abbreviations: IAD, intracranial artery dissection; DWI, diffusion weighted imaging; MRA, magnetic resonance angiograpgy; DSA, digital subtraction angiography; HR-MRI, high-resolution magnetic resonance images; CE-T1, T1 weighted image.

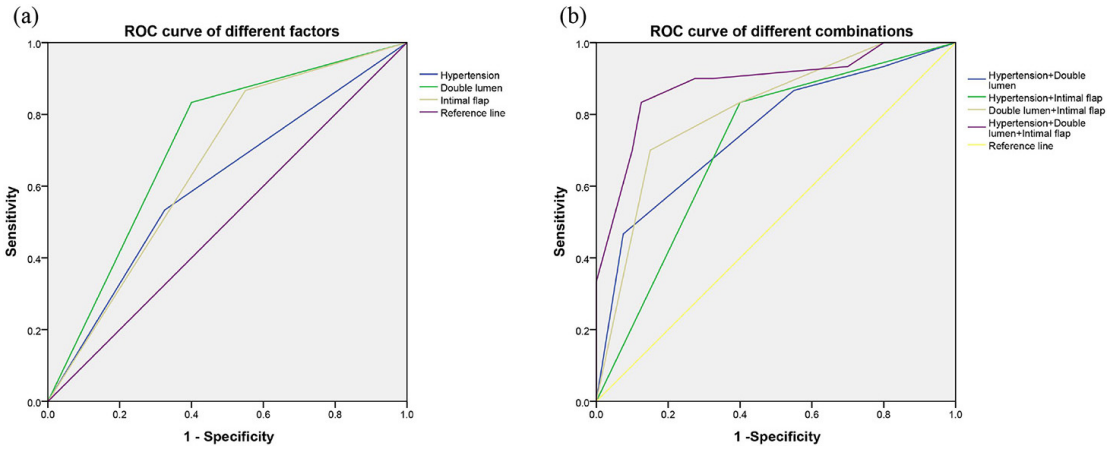

Fig. 4. ROC curves of the statistically different factors related to culprit and non-culprit lesions. (a) The ROC curve of independent factors. The AUCs were 0.604, 0.671 and 0.658 for hypertension, double lumen and intimal flap respectively. (b) The ROC curve of different combinations. The AUCs of hypertension + double lumen, hypertension + intimal flap, double lumen + intimal flap, and hypertension + double lumen + intimal flap were 0.753, 0.717, 0.811 and 0.866 respectively. Abbreviations: ROC, receiver operating characteristic; AUCs, area under curves.

detected the abnormal signal of the third cranial nerve in patients with giant cell arteritis by using HR-MRI [26]. It was found that the sensitivity, specificity, positive and negative predictive values of the abnormal signal were 0.88, 1, 1 and 0.99, respectively, indicating high diagnostic significance for HR-MRI in patients with this condition. According to the correlation between HR-MRI abnormalities and clinical manifestations in patients with ischemic stroke, the hypothesis that positive remodeling was an unsafe remodeling that can easily cause acute ischemic stroke had been

Table 3. Clinical characteristics and radiological features between IAD patients with culprit and non-culprit dissections.

	Culprit (n = 30)	Non-culprit (n = 40)	p value
Male/Female	21/9	28/12	1.000
Age (≥60)	19/11	24/16	0.777
Hypertension	25/5	23/17	0.021*
Hyperlipidemia	5/25	2/38	0.227
Diabetes	3/27	2/38	0.738
Drinking	6/24	4/36	0.402
Smoking	9/21	5/35	0.070
TG (mmol/L)	1.28 ± 0.55	1.40 ± 0.74	0.443
LDL (mmol/L)	2.59 ± 0.94	2.55 ± 0.87	0.886
HDL (mmol/L)	1.21 ± 0.36	1.19 ± 0.27	0.760
Confirmed by DSA	28/2	38/2	1.000
Location			0.186
MCA	3 (10.0)	2 (5.0)	
VA	19 (63.3)	33 (82.5)	
BA	7 (23.3)	4 (10.0)	
PCA	0 (0)	1 (2.5)	
ACA	1 (3.3)	0 (0)	
Lumen shape			0.849
Normal	2 (6.7)	3 (7.5)	
Stenosis	11 (36.6)	14 (35.0)	
Dilatation	15 (50.0)	22 (55.0)	
Stenosis and dilatation	2 (6.7)	1 (2.5)	
Hematoma	13 (43.3)	14 (35.0)	0.478
Hematoma signal on T1WI			0.726
No enhancement	17 (56.7)	26 (65.0)	
Isointensity	3 (10.0)	3 (7.5)	
Hyperintensity	5 (16.7)	6 (15.0)	
Hypointensity	5 (16.7)	4 (10.0)	
Heterogeneous intensity	0 (0)	1 (2.5)	
Double lumen	29 (96.7)	29 (72.5)	0.008*
Intimal flap	29 (96.7)	30 (75.0)	0.033*
Thrombus enhancement	7 (23.3)	13 (43.3)	0.401
Intimal flap enhancement	27 (90.0)	35 (87.5)	1.000
Vessel wall enhancement grade			0.423
No enhancement	0 (0)	0 (0)	
Enhancement	4 (13.3)	2 (5.0)	
Obvious enhancement	26 (86.7)	38 (95.0)	

Notes: *: $p < 0.05$ was set as statistical level. Abbreviations: IAD, intracranial artery dissection; TG, triglycerides; LDL, low density lipoprotein; HDL, high density lipoprotein; DSA, digital subtraction angiography; MCA, middle cerebral artery; VA, vertebral artery; BA, basilar artery; PCA, posterior cerebral artery; ACA, anterior cerebral artery; TIWI, T1 weighted image.

corroborated [27]. It was also proposed that HR-MRI might be a promising tool for detecting characteristics of the intracranial artery wall and revealing the relationship between ischemic stroke and the remodeling pattern after atherosclerosis. Further, HR-MRI confirmed that six months of high-dose statin treatment effectively stabilized symptomatic intracranial atherosclerotic plaques and improved the degree of vascular stenosis [28]. Based on the foregoing, we believe that HR-MRI has high application value in vascular diseases.

The typical imaging signs of IAD in HR-MRI include double lumen, intimal flap, luminal morphological changes and intermural hematoma [29]. The double lumen is a direct sign for diagnosis of IAD. The true cavity is generally narrow and accompanied by high-velocity blood flow. This presents a low signal on a MR black blood image sequence and a high signal on the bright blood sequence. However, a false cavity is generally wider and the blood flow rate is much slower. It is easy to form turbulence on a false cavity, thus showing an uneven signal on HR-MRI. The morphology of the true and false cavity shown by HR-MRI allows IAD to be distinguished from other cerebrovascular diseases. Intimal flap is another direct manifestation of the arterial interlayer, which can be used for the diagnosis of IAD [30]. It is known that DSA provides a reference standard for diagnosing IAD. However, in the DSA examination, the direct signs of artery dissection such as double lumen and intimal flap can be seen in less than 10% of IAD cases [12]. The application of black blood sequence can suppress the blood flow signal, so that the tube wall is well displayed on HR-MRI. In the T1 black blood sequence, the intimal flap located in the vascular cavity, was observed to manifest as a petal-like structure with equal or high signal. The three-dimensional black blood sequence better displays the intimal flap through multi-planar reorganization. In a previous study [31], 84.3% of IAD patients showed the presence of an intimal flap on T1WI sequence of HR-MRI. Consistent with that research, here it was found that 82.8% and 84.3% of IAD patients showed double lumen and intimal flap, respectively, on HR-MRI. There findings confirmed that HR-MRI has great potential for been used to IAD.

Lumen imaging can indicate the location of a lesion. As for luminal changes, beaded or segmental stenosis were the most common signs of IAD on DSA [32]. When the lesion is small, common lumen imaging may not be sufficiently specific and currently HR-MRI has an absolute diagnostic advantage. In IAD patients, intramural hematoma usually manifests as crescent thickening of the arterial wall with increased diameter, stenosis or occlusion of the true lumen, while the signal of intramural hematoma depends on the time of hematoma formation. The hematoma manifests high signal in the T1WI sequence after 48–72 hours of IAD, which is the same as atherosclerotic plaque hemorrhage in T1WI sequences [33]. However, the detection of intramural hematomas of IAD can be improved by use of HR-MRI and black blood technology [34]. In the current study 92.9% and 38.6% of IAD patients were respectively found to show altered lumen shape and visible hematoma on HR-MRI. Additionally, 28.6% and 88.6% of IAD patients showed enhanced thrombosis and endometrial flap

enhancement, respectively. So HR-MRI may make easy visualization possible for abnormal morphologies of artery dissection lesions in IAD patients.

An ischemic event was one of the common symptoms of IAD and in this study more than 90% of IAD patients had clinical symptoms. Since an ischemic event caused by a culprit dissection might seriously affect the prognosis of an IAD patient, finding predictive factors is of great significance. It was suggested in a previous study that hypertension was a key factor for vertebral artery dissection [35]. In accordance with previous studies, a remarkable difference was found here in the percentage of patients with hypertension, together with double lumen and intimal flap between culprit and non-culprit. The results of ROC analysis showed that the AUCs of hypertension, double lumen and intimal flap were 0.604, 0.671 and 0.658, respectively. Additionally, all AUCs of combinations of two or three factors were above 0.7, suggesting they provided high value for predicting ischemic events caused by the culprit dissection.

Nevertheless, there were limitations in this study. First of all, the simple size of patients recruited was relatively small. More patients are needed to verify the reported conclusions. Secondly, the HR-MRI technique had more requirements for both operators and patients. As the HR-MRI scan time was longer, slight movements of the patient seriously affected image quality. Further, some patients have severe motion artifacts and cannot be diagnosed. Finally, it is easy to misjudge flow artifacts as intimal flap in the area of large aneurysm or severe lumen stenosis.

5. Conclusions

In summary, HR-MRI allowed easy visualization of the blood vessel wall, which enabled visual observation of direct and indirect signs of IAD. HR-MRI not only improves the diagnostic rate of IAD, but also provides useful information for a better understanding of its pathophysiological mechanisms. Additionally, hypertension, double lumen and intimal flap were identified as the risk factors for predicting the occurrence of an ischemic event caused by the culprit dissection.

Author Contributions

QW—Conceptualization, Writing-Original Draft, Writing-Review & Editing. YL—Methodology, Formal analysis. BD—Data Curation, Visualization. XY—Conceptualization, Data Curation. ZZ—Data Curation, Resources. FO-Y—Formal analysis, Data Curation. MY—Data Curation, Visualization. YC—Formal analysis, Data Curation. XZ—Supervision, Methodology, Writing-Review & Editing.

Ethics Approval and Consent to Participate

This study was approved by the medical research ethics committee of the First Affiliated Hospital of Nanchang University (No. 2022-3-008). All individuals understood the purpose and latent risks, and signed informed consent.

Acknowledgment

Not applicable.

Funding

This research was funded Science and Technology Research Project of Jiangxi Provincial Department of Education, grant number 150246; This research was funded by Natural Science Foundation of Jiangxi Province, grant number 20192ACBL20040.

Conflict of Interest

The authors declare no conflict of interest.

References

[1] Montalvan V, Ulrich A, Wahlster S, Galindo D. Arterial dissection as a cause of intracranial stenosis: A narrative review. Clinical Neurology and Neurosurgery. 2020; 190: 105653.

[2] Shinya Y, Miyawaki S, Nakatomi H, Shin M, Teraoka A, Saito N. Hemorrhagic Onset Intracranial Artery Dissection of Middle Cerebral Artery Followed by Progressive Arterial Stenosis with Genetic Variant RNF213 p.Arg4810Lys (rs112735431). World Neurosurgery. 2020; 141: 192–195.

[3] Hassan AE, Zacharatos H, Rodriguez GJ, Suri MFK, Tariq N, Vazquez G, *et al*. Long-term Clinical and Angiographic Outcomes in Patients with Spontaneous Cervico-Cranial Arterial Dissections Treated with Stent Placement. Journal of Neuroimaging. 2012; 22: 384–393.

[4] Sikkema T, Uyttenboogaart M, Eshghi O, De Keyser J, Brouns R, van Dijk JMC, *et al*. Intracranial artery dissection. European Journal of Neurology. 2014; 21: 820–826.

[5] Debette S, Compter A, Labeyrie M, Uyttenboogaart M, Metso TM, Majersik JJ, *et al*. Epidemiology, pathophysiology, diagnosis, and management of intracranial artery dissection. The Lancet Neurology. 2015; 14: 640–654.

[6] Sikkema T, Uyttenboogaart M, van Dijk JMC, Groen RJM, Metzemaekers JDM, Eshghi O, *et al*. Clinical Features and Prognosis of Intracranial Artery Dissection. Neurosurgery. 2015; 76: 663–671.

[7] Bond KM, Krings T, Lanzino G, Brinjikji W. Intracranial dissections: A pictorial review of pathophysiology, imaging features, and natural history. The Neuroradiology Journal. 2021; 48: 176–188.

[8] Nakamura Y, Yamaguchi Y, Makita N, Morita Y, Ide T, Wada S, *et al*. Clinical and Radiological Characteristics of Intracranial Artery Dissection Using Recently Proposed Diagnostic Criteria. Journal of Stroke and Cerebrovascular Diseases. 2019; 28: 1691–1702.

[9] Lama S, Dolati P, Sutherland GR. Controversy in the Management of Lenticulostriate Artery Dissecting Aneurysm: a Case Report and Review of the Literature. World Neurosurgery. 2014; 81: 441.e1–441.e7.

[10] Ali MS, Amenta PS, Starke RM, Jabbour PM, Gonzalez LF, Tjoumakaris SI, *et al*. Intracranial Vertebral Artery Dissections: Evolving Perspectives. Interventional Neuroradiology. 2012; 18: 469–483.

[11] Takano K, Yamashita S, Takemoto K, Inoue T, Kuwabara Y, Yoshimitsu K. MRI of intracranial vertebral artery dissec-

tion: evaluation of intramural haematoma using a black blood, variable-flip-angle 3D turbo spin-echo sequence. Neuroradiology. 2013; 55: 845-851.
[12] Mohan IV. Current Optimal Assessment and Management of Carotid and Vertebral Spontaneous and Traumatic Dissection. Angiology. 2014; 65: 274–283.
[13] Meng Y, Dou L, Wang C, Kong D, Wei Y, Wu L, *et al*. Spinal cord infarction presenting as Brown-Séquard syndrome from spontaneous vertebral artery dissection: a case report and literature review. BMC Neurology. 2019; 19: 321.
[14] Matouk CC, Cord BJ, Yeung J, Malhotra A, Johnson MH, Minja FJ. High-resolution Vessel Wall Magnetic Resonance Imaging in Intracranial Aneurysms and Brain Arteriovenous Malformations. Topics in Magnetic Resonance Imaging. 2016; 25: 49–55.
[15] Chalian M, Behzadi AH, Williams EH, Shores JT, Chhabra A. High-Resolution Magnetic Resonance Neurography in Upper Extremity Neuropathy. Neuroimaging Clinics of North America. 2014; 24: 109–125.
[16] Kanoto M, Hosoya T. Diagnosis of Intracranial Artery Dissection. Neurologia Medico-Chirurgica. 2016; 56: 524–533.
[17] Hwang JW, Jung JM, Cha JH, Jung IE, Park MH, Kwon DY, *et al*. Using the region of interest from time-of-flight magnetic resonance angiography to differentiate between intracranial aArterial dissection and true atherosclerotic stenosis. Cerebrovascular Diseases. 2019; 47: 8–14.
[18] Cho SJ, Jung SC, Suh CH, Lee JB, Kim D. High-resolution magnetic resonance imaging of intracranial vessel walls: Comparison of 3D T1-weighted turbo spin echo with or without DANTE or iMSDE. PLoS ONE. 2019; 14: e0220603.
[19] Ortiz J, Ruland S. Cervicocerebral artery dissection. Current Opinion in Cardiology. 2015; 30: 603–610.
[20] Ryu C, Kwak H, Jahng G, Lee HN. High-Resolution MRI of Intracranial Atherosclerotic Disease. Neurointervention. 2014; 9: 9.
[21] Shin J, Chung J, Park MS, Lee H, Cha J, Seo W, *et al*. Outcomes after ischemic stroke caused by intracranial atherosclerosis vs dissection. Neurology. 2018; 91: e1751–e1759.
[22] Yu L, Zhang Q, Shi Z, Wang M, Zhang D. High-resolution Magnetic Resonance Imaging of Moyamoya Disease. Chinese Medical Journal. 2015; 128: 3231–3237.
[23] Wang G, Chen Y, Feng X, Feng P. Diagnostic value of HR-MRI and DCE-MRI in unilateral middle cerebral artery inflammatory stenosis. Brain and Behavior. 2020; 10: e01732.
[24] de Havenon A, Mossa-Basha M, Shah L, Kim S, Park M, Parker D, *et al*. High-resolution vessel wall MRI for the evaluation of intracranial atherosclerotic disease. Neuroradiology. 2017; 59: 1193–1202.
[25] Ryoo S, Cha J, Kim SJ, Choi JW, Ki C, Kim KH, *et al*. High-Resolution Magnetic Resonance Wall Imaging Findings of Moyamoya Disease. Stroke. 2014; 45: 2457–2460.
[26] Mournet S, Sené T, Charbonneau F, Poillon G, Vignal C, Clavel G, *et al*. High-resolution MRI demonstrates signal abnormalities of the 3rd cranial nerve in giant cell arteritis patients with 3rd cranial nerve impairment. European Radiology. 2021; 31: 4472–4480.
[27] Zhang DF, Chen YC, Chen H, Zhang WD, Sun J, Mao CN, *et al*. A High-Resolution MRI Study of Relationship between Remodeling Patterns and Ischemic Stroke in Patients with Atherosclerotic Middle Cerebral Artery Stenosis. Frontiers in Aging Neuroscience. 2017; 9: 140.
[28] Chung J, Cha J, Lee MJ, Yu I, Park M, Seo W, *et al*. Intensive Statin Treatment in Acute Ischaemic Stroke Patients with Intracranial Atherosclerosis: a High-Resolution Magnetic Resonance Imaging study (STAMINA-MRI Study). Journal of Neurology, Neurosurgery & Psychiatry. 2020; 91: 204–211.
[29] Lee S, Kim K, Jung J. High-resolution magnetic resonance imaging for the follow-up of intracranial arterial dissections. Acta Neurologica Belgica. 2021; 121: 1599–1605.
[30] Fukuma K, Ihara M, Tanaka T, Morita Y, Toyoda K, Nagatsuka K. Intracranial Cerebral Artery Dissection of Anterior Circulation as a Cause of Convexity Subarachnoid Hemorrhage. Cerebrovascular Diseases. 2015; 40: 45–51.
[31] Han M, Rim N, Lee JS, Kim SY, Choi JW. Feasibility of high-resolution MR imaging for the diagnosis of intracranial vertebrobasilar artery dissection. European Radiology. 2014; 24: 3017–3024.
[32] Asaithambi G, Saravanapavan P, Rastogi V, Khan S, Bidari S, Khanna AY, *et al*. Isolated middle cerebral artery dissection: a systematic review. International Journal of Emergency Medicine. 2014; 7: 44.
[33] Mizutani T, Kojima H, Asamoto S, Miki Y. Pathological mechanism and three-dimensional structure of cerebral dissecting aneurysms. Journal of Neurosurgery. 2001; 94: 712–717.
[34] Edjlali M, Roca P, Rabrait C, Naggara O, Oppenheim C. 3D Fast Spin-Echo T1 Black-Blood Imaging for the Diagnosis of Cervical Artery Dissection. American Journal of Neuroradiology. 2013; 34: E103–E106.
[35] Shi Z, Tian X, Tian B, Meddings Z, Zhang X, Li J, *et al*. Identification of high risk clinical and imaging features for intracranial artery dissection using high-resolution cardiovascular magnetic resonance. Journal of Cardiovascular Magnetic Resonance. 2021; 23: 74.